

Editors

Thomas M. Moses | Shane F. McClure

DIAMOND

Examination of the Largest Canadian Diamond

With the first major discoveries made 25 years ago, diamond mining in Canada is relatively new. The Diavik mine, located in the Northwest Territories about 300 km (190 miles) northeast of Yellowknife, began production in 2003. Today Diavik is Canada's largest diamond mine by volume, producing approximately six to seven million carats of gem-quality diamonds annually (see the lead article of this issue, pp. 104–131). Much has been reported about Diavik's extensive efforts to ensure the long-term protection of the land, water, and wildlife that are integral to local traditions and daily life in the Northwest Territories.

Adding to the significance of the Diavik mine was the spring 2015 recovery of the largest rough diamond ever found in Canada. GIA's laboratory in New York recently had the opportunity to study this historic stone. The rough weighed 187.66 ct and measured 36.96 × 32.99 × 16.80 mm. Under standard color grading lighting conditions, it appeared pale yellow (figure 1). One side of the diamond displayed clear iridescent color band-



Figure 1. This pale yellow type Ia “cape” diamond from the Diavik mine, weighing 187.66 ct, is the largest Canadian diamond to date.

ing due to light interference along the cleavage planes (figure 2, left). The stone showed irregular morphology, with a tabular shape, and was dominated by cleavage faces. Some original faces with dissolution pits were clearly visible (figure 2, center).

When observed under a gemological microscope, the irregular surface etching limited our ability to see clearly into all areas of the diamond. A dark mineral inclusion was noted near one side of the rough (figure 2, right), but little else was readily apparent. Crossed polarizing plates did

not reveal any areas of strain. The stone exhibited moderate blue fluorescence to long-wave UV radiation and faint yellow fluorescence to short-wave UV; no phosphorescence was observed. Absorption spectroscopy in the infrared region revealed that it was a type Ia diamond with a very high concentration of nitrogen. A weak hydrogen-related absorption at 3107 cm^{-1} was also recorded. UV-visible absorption spectroscopy, performed at liquid nitrogen temperature, showed typical “cape” lines, with clear absorption peaks at

Editors' note: All items were written by staff members of GIA laboratories.

GEMS & GEMOLOGY, Vol. 52, No. 2, pp. 188–197.

© 2016 Gemological Institute of America



Figure 2. Iridescent color can be seen along the cleavage plane on one side of the stone (left). Dissolution pits are observed on the surface of the yellow rough (center), and a dark mineral inclusion is clearly visible near the surface (right). Field of view 14.52 mm (left), 4.79 mm (center), and 7.19 mm (right).

415 and 478 nm. No other absorption was detected in the UV-Vis region. These gemological and spectroscopic observations confirmed that this was a natural, untreated diamond.

The diamond, named the Diavik Foxfire, will undergo further scrutiny during the cutting process, in which it will be carefully designed, shaped, faceted, and polished. It will be interesting to see if the rough yields a significant main diamond or is cut into several smaller gems.

John King, Kyaw Soe Moe, and Wuyi Wang

Natural Colorless Type IIa Diamond With Bright Red Fluorescence

The nitrogen-vacancy (NV) center is produced in nitrogen-bearing diamond through the combination of a single nitrogen atom and a vacancy. It can exist in neutral (NV⁰) and negatively charged (NV⁻) states. Using photoluminescence (PL) spectroscopy, NV centers can be detected by the occurrence of zero-phonon lines (ZPL) at 575 nm for NV⁰ and 637 nm for NV⁻. In natural type IIa diamonds, the emissions of NV centers are usually weak, and the relative intensity of NV⁰ (575 nm) is typically stronger than that of NV⁻ (637 nm). As a result, the vast majority of natural type IIa diamonds show blue fluorescence, attributed to the occurrence of defects such as N3 or dislocations, when excited by the short-wave UV radiation of the DiamondView. Recently, however, the Bangkok laboratory examined a natural colorless type IIa diamond that showed very bright red

fluorescence due to high concentrations of NV centers.

This 0.40 ct round brilliant diamond received a D color grade and an SI₁ clarity grade based on surface-reaching fractures at the girdle and on the pavilion (figure 3). The infrared absorption spectrum confirmed a type IIa diamond with no measurable defect-related absorptions. Microscopic examination with cross-polarized light revealed a relatively strong tatami strain pattern with a weak interference color (figure 4). Further examination with the Di-

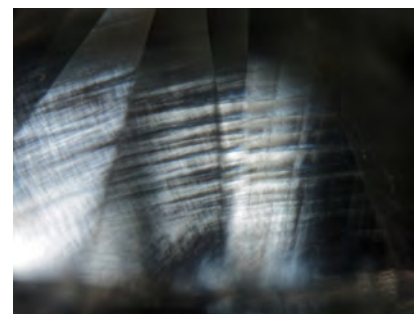
Figure 3. This 0.40 ct, D-color type IIa round brilliant diamond showed very bright red fluorescence due to strong emission peaks from the nitrogen-vacancy centers.



iamondView showed that this stone exhibited an unusual red fluorescence (figure 5), similar to that of nitrogen-doped CVD synthetic diamonds. However, the DiamondView images revealed dislocation networks of typical natural type IIa diamond along with a tree-ring growth pattern, which is very rare for natural type IIa diamond but typical for natural type Ia diamond.

In order to detect any possibility of treatment, we employed PL spectroscopy at liquid nitrogen temperature with several laser excitations. With 514 nm laser excitation, the PL spectrum revealed very strong emission peaks from NV⁰ (575 nm) and NV⁻ (637 nm) (figure 6). This is very rare in natural type IIa diamonds. The higher intensity of the NV⁰ emission was observed. For this diamond, short-wave UV excitation

Figure 4. Viewing the diamond under cross-polarizing filters revealed a tatami strain pattern with a weak interference color, a characteristic of natural growth. Field of view 3.1 mm.



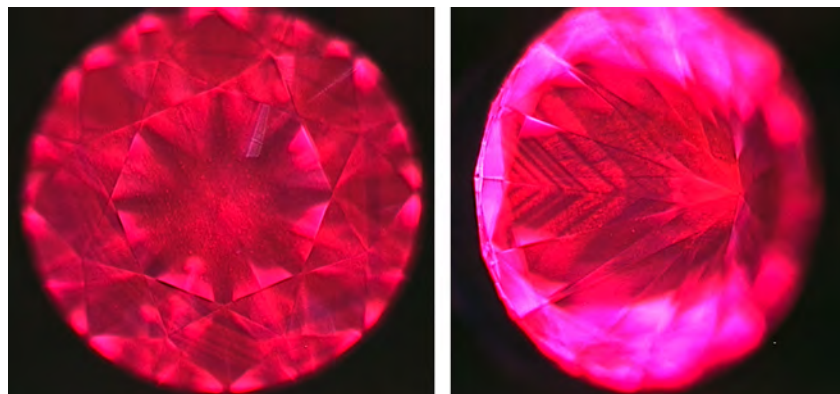


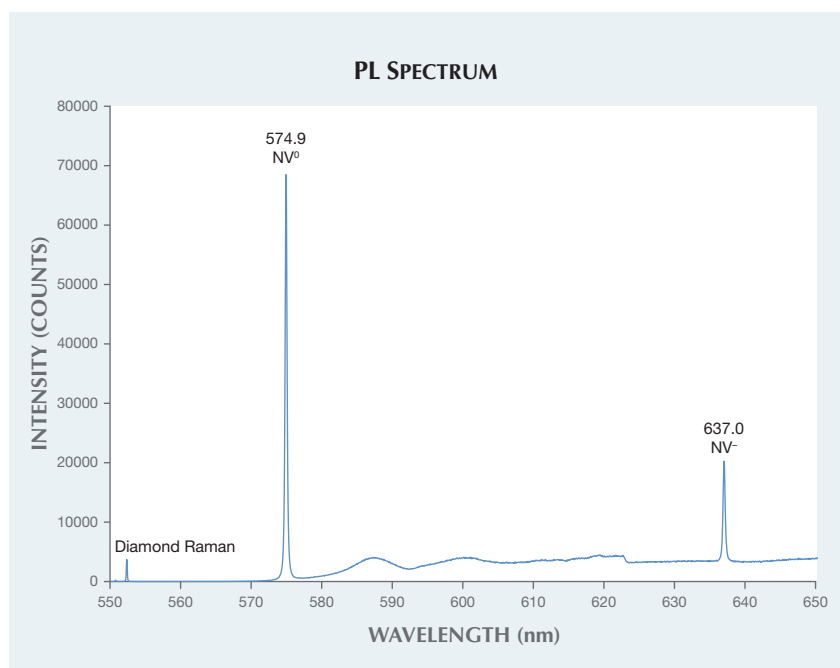
Figure 5. DiamondView images of the 0.40 ct diamond showed red fluorescence, which is unusual for natural type IIa stones. This red fluorescence was related to the intense emissions of the NV centers. Also observed was a dislocation network typical of natural type IIa diamond, along with a tree-ring growth pattern.

close to 230 nm was very effective in exciting fluorescence from the NV⁻, which has a ZPL at 637.0 nm and its strong side bands at longer wavelengths. Due to the relatively high

concentration of the NV⁻ defect, strong red fluorescence was observed.

Both spectroscopic and gemological features clearly indicated a natural

Figure 6. The photoluminescence spectrum at liquid nitrogen temperature using 514 nm laser excitation displayed strong emission peaks at 575 and 637 nm due to NV⁰ and NV⁻ centers, respectively. In natural type IIa diamonds, the intensity of NV centers is usually weaker than the diamond Raman peak at 552 nm.



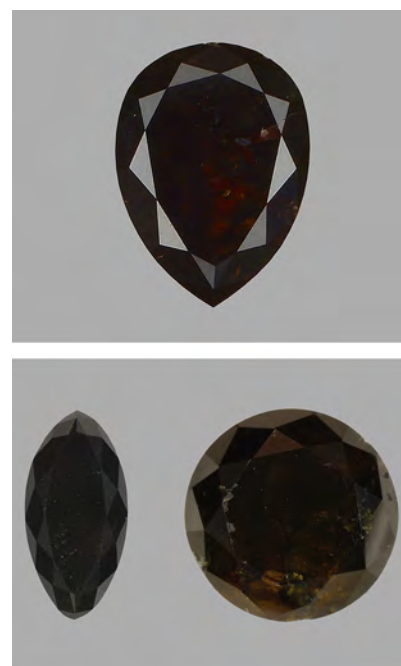
diamond. The excellent color and the red fluorescence, which is rare for a natural colorless type IIa diamond, make this a notable stone.

Wasura Soonthornantikul and
Wuyi Wang

Separation of Black Diamond from NPD Synthetic Diamond

In two recent Lab Notes, we reported on a new type of synthetic diamond: nano-polycrystalline synthetic diamond, known as NPD (Spring 2014, pp. 69–71; Winter 2014, pp. 300–301). Submitted for identification in April 2016 was a 0.70 ct pear-shaped Fancy black diamond (figure 7). The diamond's infrared absorption spectrum was strikingly similar to that of the two NPD identified specimens mentioned above. It displayed very similar absorption peaks in the one-phonon region (figure 8), which can probably

Figure 7. The 0.70 ct Fancy black pear-shaped diamond in the top photo closely resembled two NPD synthetic diamonds submitted earlier (the 1.51 ct round and 0.9 ct marquise, bottom).



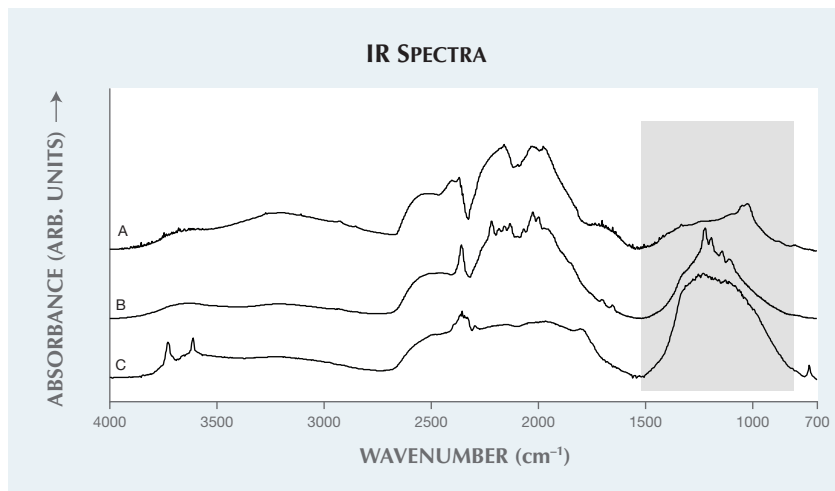


Figure 8. IR spectra of the three black samples (offset for clarity) show unusual broad peaks in the 760–1500 cm⁻¹ region (highlighted in gray): 0.70 ct natural black diamond (A), 1.51 ct NPD (B), and 0.90 ct NPD (C).

be attributed to nitrogen.

Microscopic examination revealed an abundance of dark graphitized crystal and fracture inclusions, features often associated with black gem-quality diamonds but not unlike those observed in the NPD samples (figure 9). The challenge for gem laboratories, then, is how to separate black NPD synthetic diamonds from their natural black diamond counterparts.

DiamondView imaging offers a quick and definitive solution to this problem. NPD synthetic diamond has a distinct fluorescence pattern and structure that are obvious in the DiamondView images (figure 10). This technique can provide an instant positive identification for NPD synthetic

diamond, which can be supported with further testing.

The 0.70 ct pear-shaped diamond was issued a report with a Fancy black color grade and a natural origin of color.

Paul Johnson and Kyaw Soe Moe

Unique Drilled EMERALD

A 3.39 ct emerald, as confirmed by standard gemological testing, was received by the New York lab (figure 11). At first glance it appeared to be a typical emerald with moderate clarity enhancement. It was categorized as F2, indicating that the fracturing present in the stone had a noticeable but not significant effect on the face-up

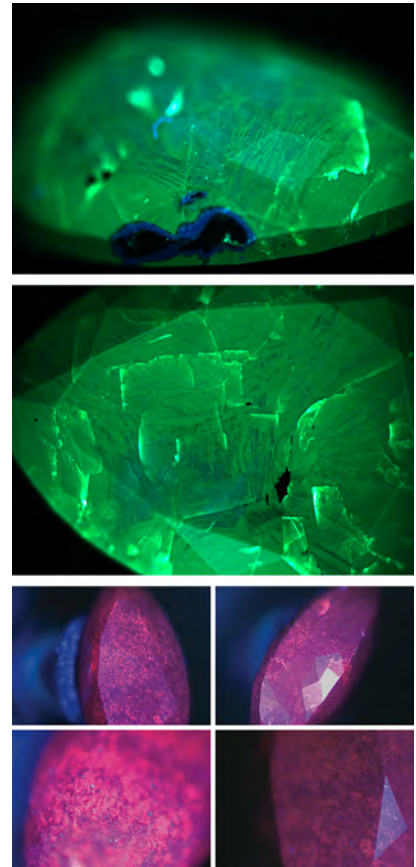


Figure 10. These DiamondView images show the fluorescence pattern and color for natural diamond (top and center) and NPD synthetic diamond (bottom).

Figure 9. Natural inclusions in black diamond (left) are compared with various inclusions previously observed in NPD synthetic diamond (center and right). Field of view 6.24 mm (left) and 1.76 mm (center and right).



appearance. Further microscopic examination of the pavilion revealed two prominent drill holes filled with

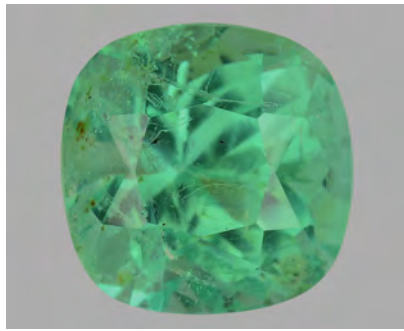


Figure 11. This 3.39 ct emerald (8.91 × 8.87 × 7.61 mm) is moderately clarity enhanced, obscuring two drill holes (not visible in this photo).

a resin and emerald fragments (figure 12). The resin displayed a blue and yellow flash effect, and gas bubbles trapped in the resin were also present (figure 13). The filler had much higher relief than the emerald host and was clearly visible under reflected light due to the difference in luster between the two materials (figure 14).

The question arose as to why such a treatment would be performed on this stone. Microscopic observation did not yield any clues. One hypothesis would be that eye-visible inclusions were removed by drilling, analogous to the laser-drilling treatment well known in diamonds. Assuming this theory is true, the “enhancement” actually significantly reduced the value of this good-quality emerald. We concluded that the stone contained a resinous material in the drill holes

Figure 12. With microscopic examination, the circular outline of the drill hole is apparent on the pavilion facet of the emerald. Field of view 4.08 mm.

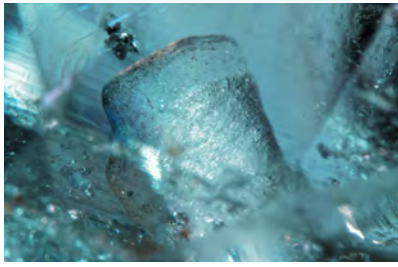


Figure 13. This drill hole shows a blue and orange flash effect along the interface between the emerald and the resin filler. Field of view 3.57 mm.

along with emerald fragments. This was the first time GIA’s New York lab had witnessed this type of enhancement in an emerald.

Edyta J. Banasiak

ORGANIC MATERIALS

Natural Blisters with Partially Filled Areas

Natural blisters and blister pearls have been the subject of previous reports in *G&G* (see Lab Notes from Fall 1992, Spring 1995, Winter 1996, and Winter



Figure 14. Examination of the drill hole in reflected light shows an emerald fragment intentionally placed in the opening, presumably to conceal the hole. Note the luster difference between the emerald and the resin filler. Field of view 3.57 mm.

2015, and Gem News International from Fall 2001 and Winter 2009). In February 2016, four large “pearls” (figure 15) were submitted to GIA’s Bangkok laboratory for identification. On first impression they appeared to differ from most pearls or blister pearls examined in the past. The specimens ranged from approximately 25.06 × 18.31 × 13.41 mm to 55.90 × 13.89 × 7.96 mm, and they weighed 32.33,

Figure 15. The four large baroque blisters examined are shown alongside a *Pinctada maxima* shell (left), a *Pteria sterna* shell (second from the left) and two *Pteria penguin* shells.





Figure 16. Dark and cream-colored bands on the bases appeared to be organic-rich formations.

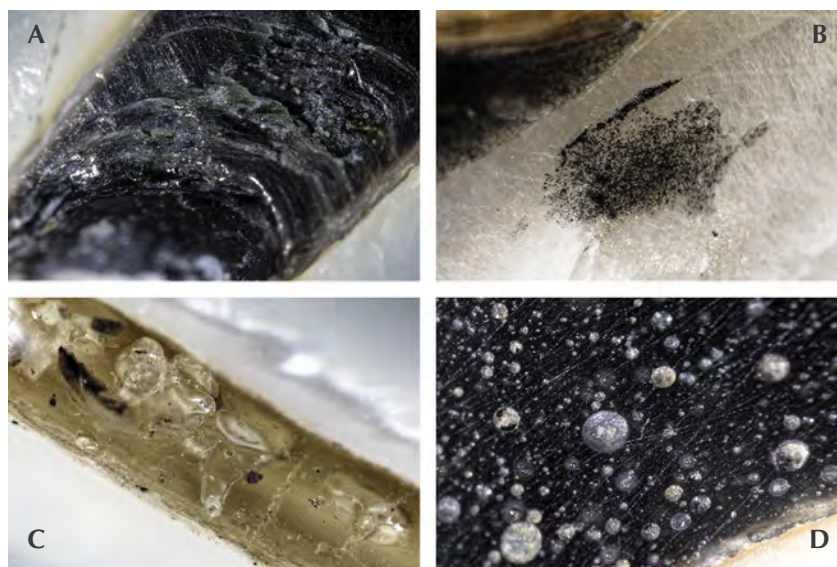
37.20, 41.41, and 52.17 ct. Two of the items were white, and the other two were silver and orangy brown.

All the samples had eye-visible areas on their bases and around their outlines where they had obviously been worked or cut to either remove them from their shell hosts or improve the symmetry (in some cases both). These are telltale signs of blisters and blister pearls, since both must be removed from the shell to be presented in loose form. What caught

our attention was the fact that all four items possessed dark or cream bands on their bases (figure 16). These bands appeared to be organic-rich formations, noted in some pearls and more commonly in shells, yet this did not turn out to be the case in three of the samples.

The items were considered blisters rather than blister pearls (E. Strack, *Pearls*, Ruhle-Diebener-Verlag, Stuttgart, Germany, 2006, pp. 115–127). This determination was based on ex-

Figure 17. A: Part of the dark conchiolin-rich curving band on the flat base of the 32.33 ct white blister; field of view 2.88 mm. B: Black pinpoint particles in the transparent near-colorless filler on the base of the 37.20 ct colored blister; field of view 1.20 mm. C: Distorted bubbles in the transparent filler on the base of the 41.41 ct white blister; field of view 2.40 mm. D: Obvious bubbles in the filler on the base of the 52.17 ct colored blister; field of view 2.40 mm.



ternal appearance and features, the “work” that had taken place on them in relation to where they were likely removed from the shells, and the results of real-time X-ray microradiography (RTX), which revealed growth arcs following the shape of the blisters to varying degrees.

The curving black band on the base of the smallest white blister contained translucent to opaque organic-looking material characteristic of conchiolin (figure 17A), one of the constituents of pearls and shells. The remaining three blisters had structures within their bands that did not match the structure observed in the first blister. The bands in the two orangy brown blisters consisted of an essentially transparent near-colorless substance in which minute black pinpoint particles imparted an overall black color (figure 17B). Meanwhile, the band in the remaining white blister showed areas of completely transparent near-colorless material and other areas of the same near-colorless material, mixed with small pieces of what appeared to be shell fragments. Distorted bubbles were clearly visible in the transparent areas on the base of the partially filled white blister (figure 17C) and one of the colored blisters (figure 17D); no obvious bubbles were seen in the other blister. RTX also revealed the extent of the filling on the bases of the three blisters.

Raman spectroscopy of the near-colorless filled areas of the two colored blisters did not show any polymer or resin peaks that matched those found in the white blister’s filling. Therefore, we conducted basic testing on all three samples with a very carefully placed hot point in areas of the filling where some damage or abrasion already existed. The unmistakable plastic odor and melting of the tested areas was enough to confirm the artificial nature of the fillers. Interestingly enough, the fillers did not display a noticeable fluorescence under long-wave or short-wave ultraviolet light, but the two orangy brown blisters did exhibit distinct orange to orange-red fluorescence, which is characteristic of the

porphyrins (naturally occurring pigments) known to exist in *Pteria* species shells of similar coloration (L. Kiefert et al., "Cultured pearls from the Gulf of California, Mexico," Spring 2004 *G&G*, pp. 26–38). Out of curiosity, we also checked the dark conchiolin-rich band in the smaller white blister with the hot point and fluorescence. It was no surprise to smell a distinctly unpleasant organic reaction from the band and see a weak chalky yellowish reaction under UV lighting.

These four blisters were good examples of this material, and three of them were the first partially filled blisters to be examined by GIA's Bangkok laboratory. The three partially filled blisters show that even material with relatively low market value may be treated in some way, and buyers should always be aware of what is being offered to them.

Areeya Manustrong

Unusual Yellowish Green SPINEL

Gem-quality spinel (MgAl_2O_4) occurs in a variety of colors based on the trace elements present within the stone. While synthetic spinels are available in almost any color, some colors are rarely found in natural spinel. The New York lab received a 2.54 ct light yellowish green spinel with unusually strong green fluorescence (figure 18). This variety of color, along with the strong fluorescence (in both long-wave and short-wave UV radiation) is rare in natural spinel, and we needed proof that this stone was not synthetic.

A refractive index of 1.715 suggested the stone might be natural (flame-fusion synthetic spinels typically have an RI of 1.728). Microscopic examination revealed a very small fingerprint shallow to the table facet. While not conclusively diagnostic for natural origin, it supported the possibility. When observed under cross-polarized filters, the stone revealed very little strain, more consistent with a natural spinel. To confirm natural origin, PL spectra and trace element chemistry data were collected.

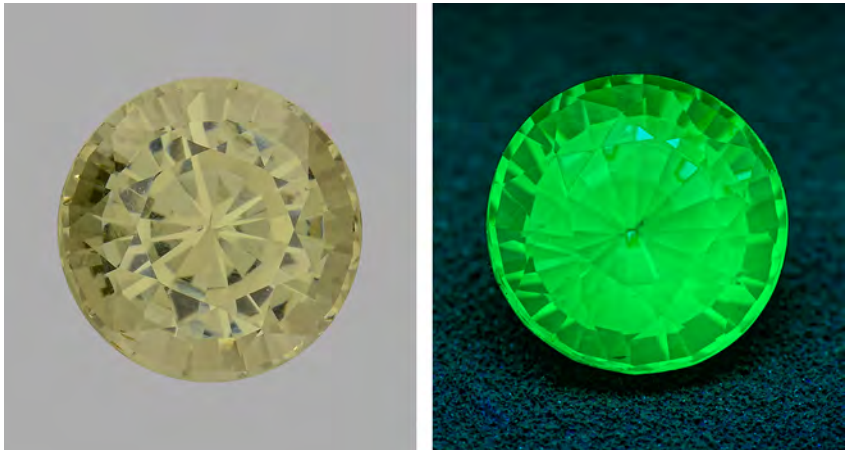


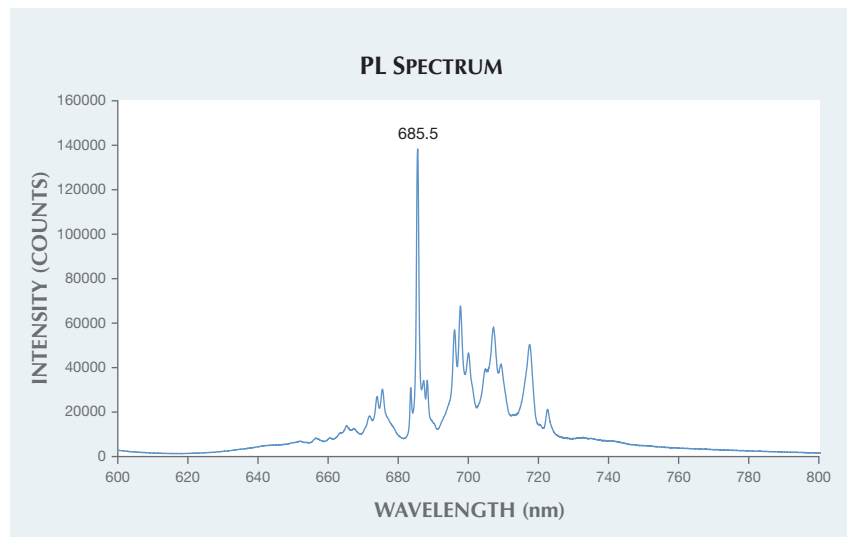
Figure 18. This 2.54 ct yellowish green spinel is shown under daylight conditions (left) and short-wave UV light (right).

The PL spectra were collected at room temperature, using 514 nm laser excitation. The sharp and defined chromium emission features, with the strongest peak at approximately 685.5 nm (figure 19), verified that the stone was natural and unheated (S. Saeseaw et al., "Distinguishing heated spinels from unheated natural spinels and from synthetic spinels," 2009, <http://www.gia.edu/gia-news-research-NR32209A>). Heat treatment typically broadens and shifts the posi-

tion of PL peaks (a similar effect is seen in synthetic spinels). Using laser ablation-inductively coupled plasma-mass spectrometry (LA-ICP-MS), high concentrations of natural trace elements were measured—particularly lithium, gallium, zinc, and beryllium. This reinforced our finding that the spinel was natural.

The stone also exhibited relatively high levels of manganese and iron. Fe can play various roles as a chromophore in spinel, depending on coor-

Figure 19. Well-defined chromium emission features in the photoluminescence spectrum confirm natural, unheated spinel.



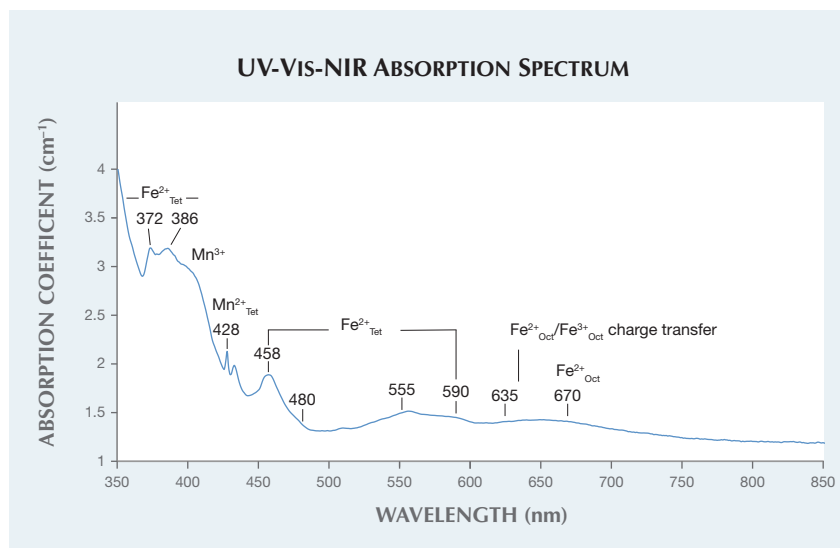


Figure 20. In the spinel's UV-Vis-NIR absorption spectrum, the combination of iron and manganese peaks produces a transmission window in the green region of the visible spectrum.

dination within the crystal structure (divalent substitution of Mg and trivalent or divalent substitution of Al), but it is mostly responsible for different shades of blue and greenish blue (V. D'Ipollito et al., "Color mechanisms in spinels: cobalt and iron interplay for the blue color," *Physics and Chemistry of Materials*, Vol. 42, 2015, pp. 431–439, <http://dx.doi.org/10.1007/s00269-015-0734-0>). Mn (divalent substitution of Mg and trivalent substitution of Al) is known to act as a yellow chromophore (among other colors) in spinels (F. Bosi et al., "Structural refinement and crystal chemistry of Mn-doped spinel: a case for tetrahedrally coordinated Mn^{3+} in an oxygen-based structure," *American Mineralogist*, Vol. 92, 2007, pp. 27–33, <http://dx.doi.org/10.2138/am.2007.2266>). The combination of Fe and Mn within the crystal structure provided a transmission window in the green region of the visible spectrum (figure 20). Using a charge-coupled device (CCD) detector and a long-wave UV light source, the green fluorescence emission band was calculated to be centered at approximately 520 nm. This luminescence was attributed to Mn^{2+} cations (Summer 1991 Lab Notes, pp. 112–113). The fluorescence could have contributed to the overall

color of the stone by adding more green hue through emission.

This was one of the most unusual colors of spinel examined by GIA.

Akhil Sehgal and Daniel Girma

SYNTHETIC DIAMOND

Large Blue and Colorless HPHT Synthetic Diamonds

The technology for producing gem-quality synthetic diamonds is making rapid progress. In May 2016, GIA's

Hong Kong laboratory examined five large HPHT synthetic diamonds grown by New Diamond Technology (NDT) in St. Petersburg, Russia (table 1). Examination confirmed that all of them had the known characteristics of HPHT synthesis.

Two of the synthetic diamonds were color graded as Fancy Deep blue (figure 21). The 5.26 ct heart shape and the 5.27 ct emerald cut both surpassed the previous record for largest blue HPHT synthetic, a 5.02 ct specimen reported very recently (Spring 2016 Lab Notes, pp. 74–75). Infrared absorption spectroscopy showed that both were type IIb, with strong absorption bands from boron impurity. We observed the typical color banding of HPHT synthetics, with more blue color concentrated in the {111} growth sector. PL analysis at liquid nitrogen temperature with various laser excitations revealed no impurity-related emissions, indicating these stones were surprisingly pure in composition and lacking in defects.

The other three samples were colorless (figure 22). The largest one was a 10.02 ct emerald cut with E color equivalent. This stone was previously reported in 2015 (R. Bates, "Company grows 10 carat synthetic diamond," *JCK*, May 27, www.jckonline.com/2016/01/20/company-grows-10-carat-synthetic-diamond). The round cut

Figure 21. The largest blue HPHT synthetic diamonds to date: a 5.26 ct heart shape and a 5.27 ct emerald cut. Both were graded as Fancy Deep blue.

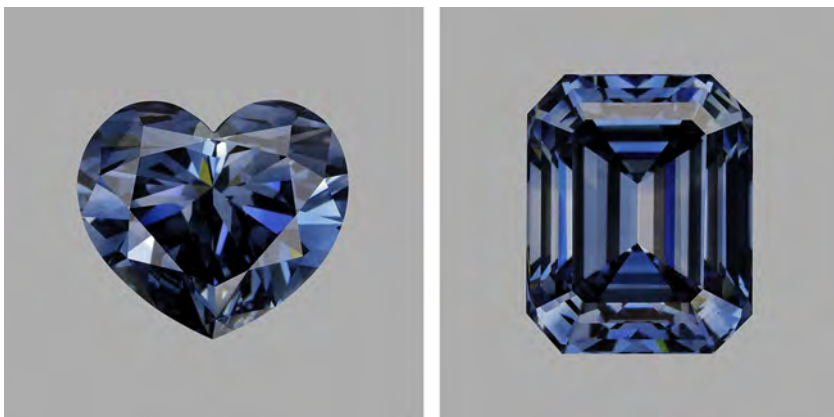


TABLE 1. Large HPHT synthetic diamonds recently examined by GIA.

Sample	Weight (ct)	Cut	Color	Clarity
1	5.26	Heart	Fancy Deep blue	VVS ₂
2	5.27	Emerald	Fancy Deep blue	VS ₁
3	10.02	Emerald	E	VS ₁
4	5.06	Round	D	VS ₂
5	5.05	Heart	D	VS ₂

weighed 5.06 ct and the heart shape 5.05 ct; both were graded as D color equivalent. Infrared absorption spectroscopy confirmed these three were type IIa diamond, but with a very weak boron-related absorption band at $\sim 2800\text{ cm}^{-1}$. PL spectroscopy revealed very weak emissions from the [Si-V] doublet at 737 nm, the Ni_i⁺ doublet at 884 nm, and NV⁰ at 575 nm.

For all five samples, multiple growth sectors were observed in DiamondView fluorescence images, showing features similar to other HPHT synthetic diamonds. Strong blue phosphorescence was also detected. Unlike natural type IIa or IIb diamonds, they showed no dislocation or strain when examined under a cross-polarized microscope, a strong indication of high-quality crystallization. Their clarity ranged from VS₂ to VVS₂, attributed to a few tiny metallic inclusions trapped during diamond growth. No fractures were observed. All of these gemological and spectroscopic features are consistent with typical HPHT synthetic diamonds. This material can be accu-

rately identified with GIA's existing protocols for analysis.

In addition to their size, these five HPHT synthetic diamonds displayed gemological features comparable to those of top-quality natural diamonds, when graded using the system for natural diamonds. This group of laboratory-grown diamonds demonstrated the quality and size HPHT growth technology has achieved. It is obvious that more and more high-quality HPHT synthetic diamonds, including those with significant size, will be introduced to the jewelry industry. GIA's decades of research into both HPHT and CVD synthetic diamonds allows for the ready identification of these synthetic diamonds.

Wuyi Wang and Terry Poon

Yellow Synthetic Diamond with Nickel-Related Green Fluorescence

Gem-quality yellow synthetic diamonds have been a part of the industry for some time now. The gemological properties used to iden-

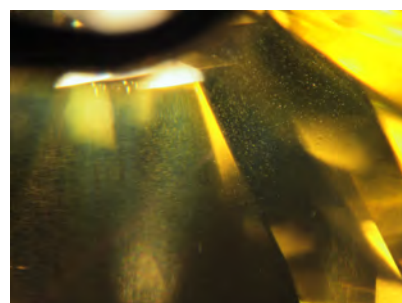


Figure 23. Under darkfield illumination, the pinpoint flux cloud is seen throughout the diamond. Field of view 3.57 mm.

tify these synthetics have been extensively documented (see J.E. Shigley et al., "A chart for the separation of natural and synthetic diamonds," Winter 1995 *G&G*, pp. 256–264).

GIA's New York laboratory recently tested a 0.99 ct synthetic diamond with Fancy Vivid yellow color, disclosed as a product of HPHT (high-pressure, high-temperature) growth, which showed some unusual gemological features. Its UV-Vis absorption spectra showed a smooth rise from 500 nm to higher energy. The mid-IR absorption spectra indicated a type I diamond with isolated nitrogen (C-center) responsible for the intense yellow color. The sample displayed a moderate greenish yellow fluorescence under long-wave UV and slightly stronger greenish yellow fluorescence under short-wave UV. It had a noticeable

Figure 22. The emerald cut on the left is the largest colorless HPHT synthetic diamond ever reported (10.02 ct, E color). The other two, a 5.06 ct round and a 5.05 heart, both had D color.



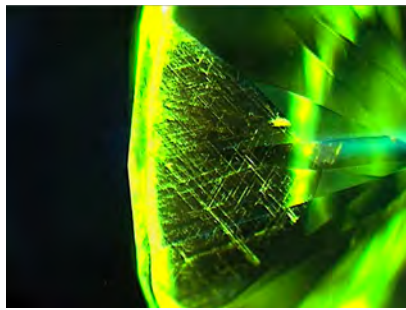


Figure 24. This DiamondView image shows the unusual green crosshatched pattern in the hour-glass structure of the HPHT-grown synthetic.

pinpoint flux cloud throughout (figure 23) and obvious yellow color zoning following the growth sectors—both characteristic gemological features of a yellow HPHT-grown synthetic diamond.

Unlike other yellow HPHT-grown synthetics, the DiamondView images showed an unusual green fluorescent crosshatched pattern within the hour-glass structure (figure 24). This closely resembles the pattern seen in natural diamonds, which means the synthetic could have easily been mistaken for a

Figure 25. Under cross-polarized light, the HPHT synthetic exhibited a mottled strain pattern with moderate birefringence colors. Field of view 4.79 mm.

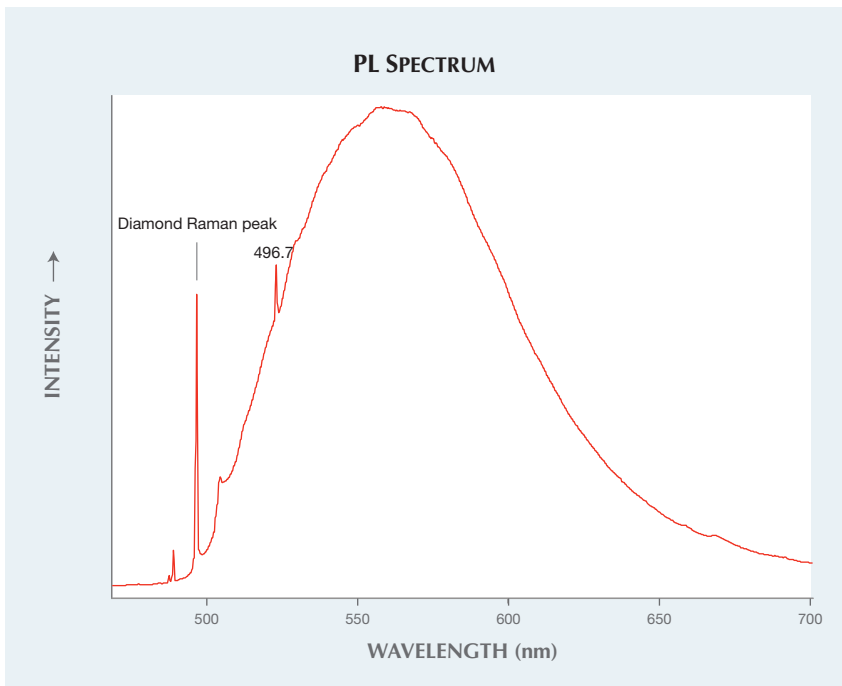
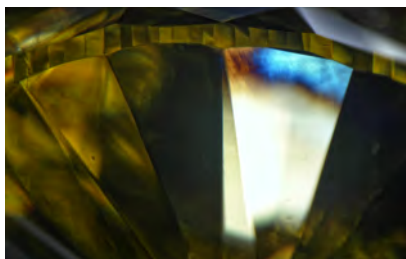


Figure 26. PL spectroscopy with blue (457 nm) laser excitation shows the S3 emission band (496.7 nm), which is responsible for the HPHT synthetic diamond's green fluorescence.

natural diamond. Under cross-polarized light, it showed a mottled strain pattern with moderate birefringence colors (figure 25). Most yellow HPHT-grown synthetics do not show a clear strain pattern and have weak birefringence colors. Further examination with PL spectroscopy using blue (457 nm) laser excitation showed that the green fluorescence was caused by the S3 defect (496.7 nm, shown in figure 26), which is due to the presence of nickel—a very unusual feature for an HPHT-grown synthetic diamond.

This yellow HPHT-grown sample with gemological features we had not seen before shows once again how synthetic diamonds can be mistaken for natural diamonds. Caution must be

taken, and careful gemological and spectroscopic analysis is essential.

Lisa Kennedy and Paul Johnson

PHOTO CREDITS:

Sood Oil (Judy) Chia—1, 11, and 18 (left); Kyaw Soe Moe—2; Nuttapol Kitdee—3; Charuwan Khowpong—4; Wuyi Wang—5; Jian Xin (Jae) Liao—7 and 18 (right); Paul Johnson—9 and 10; Edyta J. Banasiak—12, 13, and 14; Lhapsin Nillapat—15 and 16; Kwanreun Lawanwong—17; Johnny Leung—21 and 22; Lisa Kennedy—23, 24, and 25.

For online access to all issues of GEMS & GEMOLOGY from 1934 to the present, visit:

gia.edu/gems-gemology

